

# Influence of Polymerizable Surfactants on Dispersion and Mechanical Properties of Clay-Photopolymers

*Kwame Owusu-Adom, Department of Chemical & Biochemical Engineering, University of Iowa, Iowa City, IA, USA*

*Allan Guymon, Department of Chemical & Biochemical Engineering, University of Iowa, Iowa City, IA, USA*

## Introduction

Organic-inorganic nanocomposites are interesting materials that exhibit distinct advantages over conventional composites. Applications in electronic, optical and biological systems are potentially accessible from these nanocomposites.<sup>1-4</sup> One such example, polymer-clay nanocomposites, has been investigated recently due to certain unique properties afforded by incorporating small concentrations of clay into the polymer matrix. Pioneering work by Okada *et al.* demonstrated that increases in thermomechanical properties of Nylon 6/clay nanocomposites are observed when less than 10wt% clay is added to the polymer.<sup>5-7</sup> Others have shown various degrees of improvement in gas barrier, heat distortion and modulus of the nanocomposite.<sup>8-14</sup> These properties have been attributed to the nanoscale dimensions of the dispersed clay particles which facilitate significant nanoparticle-polymer interaction.

The majority of work in the field, however, has focused on dispersing clay particles in linear or very low crosslinked polymers. Photopolymers are an important class of materials that take advantage of the speed, spatial and temporal control of initiation, and energy efficiency attributes of the photopolymerization process. Coatings, thin films and dental materials are some current applications of photopolymers which may benefit from enhancements inherent to incorporating clay nanoparticles in the polymer. In addition, new materials with advanced properties could be developed from embedding clay nanoparticles in various photopolymeric materials. To realize this goal however, effective dispersion of clay particles is required. Dispersing clay particles into exfoliated domains (delaminated clay tactoids) is a critical challenge in the synthesis of polymer-clay nanocomposites. More commonly observed is the intercalated state that generally does not lead to the unique properties associated with exfoliated nanocomposites. Efforts to generate exfoliated clay nanoparticles have included thermomechanical (melt blending/extrusion),<sup>15-18</sup> solvent induced exfoliation<sup>12,19,20</sup> and chemically driven means<sup>21,22</sup> in thermally cured materials. Decker *et al* and Uhl *et al* have also examined clay-photopolymer nanocomposites.<sup>10,11</sup> The critical challenge in photopolymer nanocomposites remains exfoliation due to the nature of the photopolymerization process.

Clay dispersion occurs by two diffusion processes: polymer migration into clay interlayers and diffusion of individual clay platelets away from adjacent tactoids into the polymer network to result in exfoliated domains. For low crosslinked polymer networks, mechanical agitation or swelling may afford easier exfoliation since polymer mobility could be increased by thermal or solvent conditions. In photopolymers, especially highly crosslinked acrylate systems, inducing exfoliation during or after polymerization may be challenging since the polymer network develops very early in the polymerization process. This problem could be circumvented if monomer swells the interparticle layers followed by

polymerization within these clay interlayers. This research studies a variation of this theme by altering dispersant molecules to include reactive species used to modify clay surfaces for enhanced dispersion in organic matrices. Thiol and (meth)acrylate functional groups are incorporated into quaternary ammonium surfactants utilized for modifying clay surfaces. The influence of these reactive species on organoclay dispersion is investigated.

The objective of this paper is to elucidate the influence of polymerizable dispersants on organoclay dispersion in multifunctional acrylate monomer systems. Influence of the polymerizable organoclay on nanocomposite mechanical properties was also investigated. It is shown that modifying clay surfaces with certain polymerizable surfactants improves their dispersion in photopolymer formulations. Mechanical properties are also improved from incorporating the polymerizable organoclays.

## Experimental

### Materials

Rapid curing, low viscosity difunctional acrylate monomers tripropylene glycol diacrylate (TrPGDA), neopentyl glycol diacrylate (NPGDA) and 1,6-hexanediol diacrylate (HDDA) were obtained from Sartomer Co. (Exton, PA) and used without further purification. The photoinitiator utilized was 2,2-dimethoxy-2-phenyl acetophenone (DMPA - Ciba Specialty Chemicals). Methacrylated quaternary ammonium surfactants (C14MA and PM1) were synthesized according to procedures described in the literature.<sup>23,24</sup> These surfactants were used to form organically modified clay using cation exchange procedures.<sup>25</sup> A third polymerizable organoclay was synthesized through a Michael addition reaction of (meth)acrylated organoclay and a multifunctional thiol monomer. Sodium Montmorillonite (Cloisite Na®) with cation exchange capacity (CEC) of 92.6 meqiv/100g clay was obtained from Southern Clay Products and used in developing the polymerizable organoclays. Cloisite 15A (Southern Clay Products, Gonzalez, TX) was utilized for comparative studies. Figure 1 shows the chemical structures of the monomers and surfactants.

### Methods

Polymerizable organoclays were prepared as outlined elsewhere.<sup>25</sup> Briefly, 10g of clay was dissolved in 1000ml of de-ionized water under continuous stirring. The mixture was sonicated for one hour. Requisite amount of surfactant based on desired extent of cation exchange was dissolved in a separate beaker. The clay mixture and surfactant solution were combined and stirred continuously for 12-24 hours. The slurry was centrifuged and washed several times to remove unbound surfactants in the organoclay. The resulting organoclay was dried under vacuum overnight. Fourier transform infrared spectroscopy (FTIR, Nicolet 670) was used to confirm quaternary ammonium surfactants anchored onto clay surface by examining the presence of characteristic peaks from the surfactants.

Small angle x-ray scattering (SAXS) was utilized to characterize dispersion behavior of the various formulations. These measurements were conducted using a Nonius FR590 X-ray apparatus equipped with a Cu K $\alpha$  radiation source ( $\lambda = 1.54 \text{ \AA}$ ) at 40kV and 30mA intensity.<sup>26</sup> Rectangular bars measuring approximately 2 x 13 x 25mm were used in analyzing viscoelastic properties of the photopolymerized nanocomposites on a dynamic mechanical analyzer (DMA-Q800, TA Instruments). Young's modulus measurements were taken at room temperature with an applied dynamic force in the linear regime (less than 10% strain). A minimum of three samples were tested for each specimen, and the average value reported. Photopolymerization rates were monitored using a Perkin Elmer Diamond

differential scanning calorimeter modified with medium pressure mercury arc lamp (photo-DSC). Photopolymerization rates were normalized to the concentration of reactive species in the system to allow equal basis of comparison.<sup>27</sup>

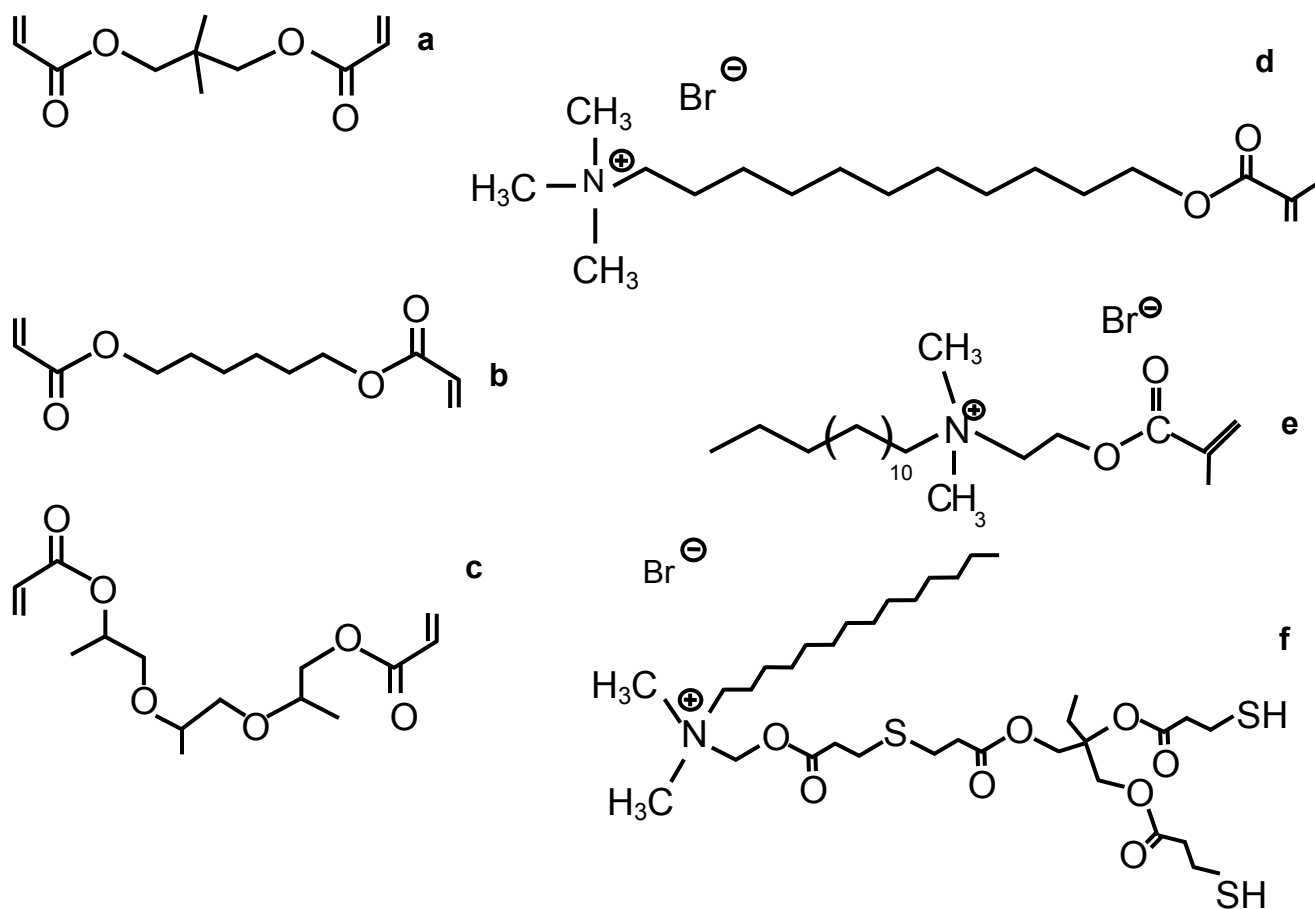


**Figure 1:** Chemical structures of monomers: a) neopentyl glycol diacrylate, NPGDA; b) 1,6-hexanediol diacrylate, HDDA; c) tri(ethylene glycol) diacrylate, TrPGDA PEGDA. Chemical structures of dispersants: d) undecylmethacryloyloxy trimethylammonium bromide, PM1; e) tetradecyldimethyl ammoniummethylmethacrylate bromide, C14MA and f) dodecyltrimethylol di(3-mercaptopropionate) dimethylammonium bromide, PSH2.

## Results and Discussion

Successfully exfoliating clay particles in polymer-clay nanocomposites typically leads to enhanced properties not attainable with conventional composite materials. Clay surfaces are typically modified with quaternary ammonium surfactants to aid dispersion in the polymer matrix. To facilitate dispersion in photopolymer-clay nanocomposites, quaternary ammonium surfactants were modified with reactive functionalities that could polymerize within the clay galleries to induce exfoliation. The reactive species also allow one to incorporate specific characteristics into the nanocomposite through the choice of surfactant chemistry. FTIR is a powerful tool for characterizing the surface modification process. An example of such characterization technique is shown in Figure 2. Figure 2a shows the absorption profiles of C14MA-organoclay and the unmodified clay. Absorption bands signifying presence of specific functional groups associated with the surfactants are evaluated. Presence of vibrational bands

for carbonyl, C=C double bonds, and methylene functional groups is used to evaluate presence of the quaternary ammonium surfactants. Absorption bands at  $1410\text{ cm}^{-1}$ ,  $1740\text{ cm}^{-1}$  and  $2845/2935\text{ cm}^{-1}$  suggest the presence of functional groups characteristic of methacrylate species on the clay surface. Michael addition of multifunctional thiol monomers to yield thiol organoclay is also characterized by the disappearance of C=C double bond absorption band at  $1410\text{ cm}^{-1}$  and appearance of a thiol peak at  $2570\text{ cm}^{-1}$  (Figure 2b).

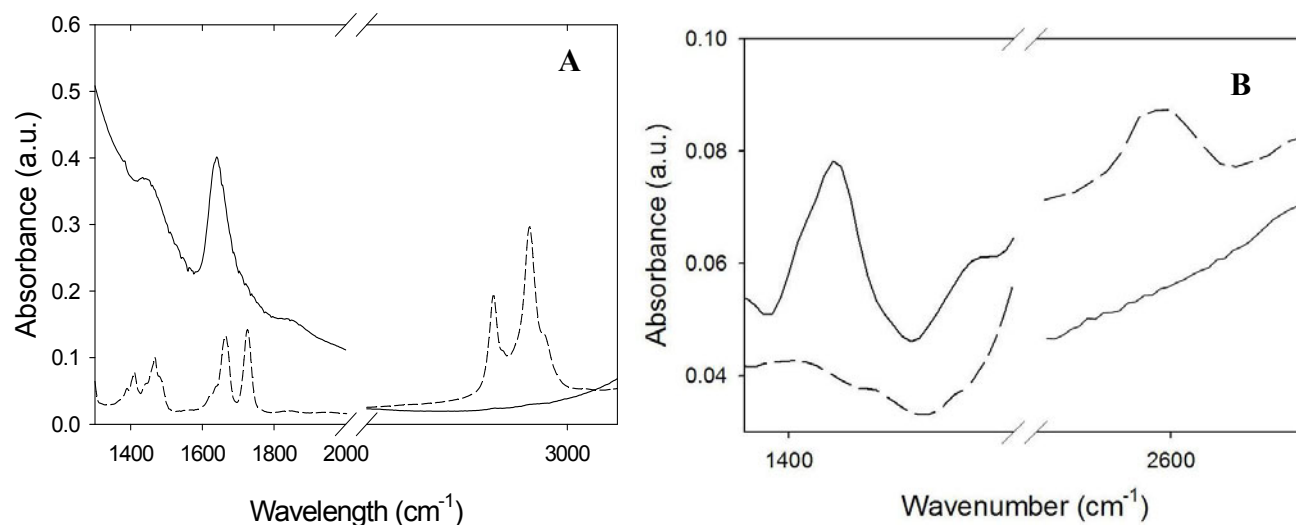


**Figure 2:** a) FTIR plots of unmodified clay (solid line) and C14MA-modified organoclay (dashed line). Absorbance peaks at  $1410\text{ cm}^{-1}$  ( $\nu_{\text{C}=\text{C}}$ ),  $1735\text{ cm}^{-1}$  ( $\nu_{\text{C}=\text{O}}$ ) and doublet peaks at  $2845$  and  $2935\text{ cm}^{-1}$  ( $\nu_{\text{CH}}$ ) indicate presence of methacrylate species on clay surface. Michael addition reaction with multifunctional thiol monomer (b) leads to disappearance of  $1410\text{ cm}^{-1}$  ( $\nu_{\text{C}=\text{C}}$ ) band and appearance of  $2570\text{ cm}^{-1}$  ( $\nu_{\text{SH}}$ )

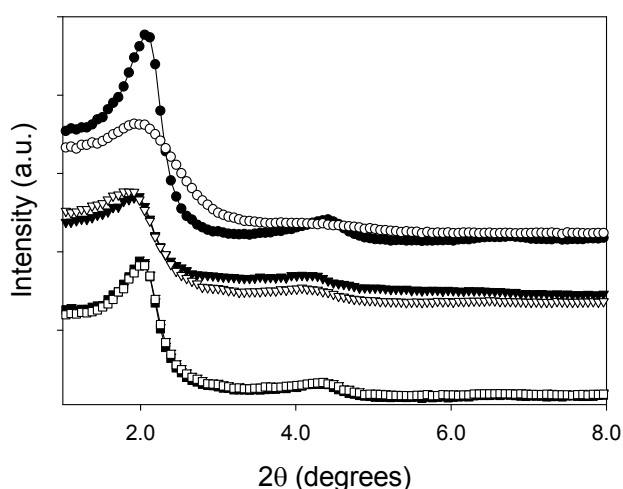


**Figure 3:** SAXS profiles of 5wt% Cloisite 15A dispersed in NPGDA (circles), HDDA (triangles) and TrPGDA (squares). Filled symbols represent uncured samples and unfilled symbols represent polymerized samples.

Small angle x-ray scattering was used to probe the dispersion behavior of organoclays in different multifunctional acrylate monomers. Using methacrylated quaternary ammonium surfactants as dispersants may enhance exfoliation in two ways. First, because of similarities in organoclay and monomer chemistries, diffusion of monomer into clay galleries could be enhanced thereby swelling the clay platelets for potentially enhanced dispersion. Secondly, polymerization of the functional groups to yield larger polymer species could also aid delamination of the organoclay particles. The dispersion behavior of 5wt% non-polymerizable organoclay dispersed in the different monomers is shown in Figure 3. Cloisite 15A has intercalated morphology in all three monomers throughout photopolymerization. In NPGDA, the non-polymerizable organoclay is highly intercalated (as shown by a well-defined peak around  $2\theta = 2.1^\circ$ ) before

photopolymerization. The peak intensity decreases after photopolymerization, and suggests formation of some exfoliated organoclay domains in the polymer matrix. The organoclay intercalates in both HDDA and TrPGDA before and after photopolymerization. However, peak intensity for HDDA is significantly lower, suggesting presence of potentially exfoliated domains in the nanocomposite. It should be emphasized however, that the non-polymerizable organoclays are all intercalated in the polymer.

In comparison, Figures 4a and 4b show SAXS profiles of polymerizable organoclays dispersed in NPGDA and HDDA respectively. The SAXS profiles of C14MA-organoclay shows a diffused peak centered on  $2\theta = 2.1^\circ$  that indicates existence of a mixture of intercalated and exfoliated domains before photopolymerization. The peak intensity decreases after polymerization and shows evidence of some exfoliation. When the position of the reactive functionality on the quaternary ammonium surfactant is changed, the resulting organoclay disperses in a completely different fashion. PM1-organoclay appears to exfoliate before photopolymerization. After photopolymerization, the exfoliated domains are retained in the polymer matrix. PSH2-organoclay partially exfoliates before photopolymerization and appears to exfoliate completely after polymerization. All the polymerizable organoclays disperse similarly in both HDDA (Figure 4b) and TrPGDA (not shown). PM1-organoclay exfoliates in the monomer in all cases. PSH2-organoclay on the other hand, disperses with small pockets of intercalated domains before polymerization. C14MA-organoclay appears to disperse into a mixture largely of intercalated domains with some exfoliation as well. Initiating polymerization leads to generation of more exfoliated domains in PSH2- and C14MA-organoclays. However, C14MA-organoclay maintains a higher degree of intercalated tactoids in all monomers investigated. In spite of the differences in dispersion behavior, it is obvious that introducing reactive functional groups into the quaternary ammonium surfactants affords enhanced dispersion in acrylated systems. It should also be noted that these organoclays disperse in a similar fashion for concentrations up to 5wt%. The higher amount of exfoliated domains could be related to monomer-dispersant compatibility and intragallery polymerization of the reactive surfactants.

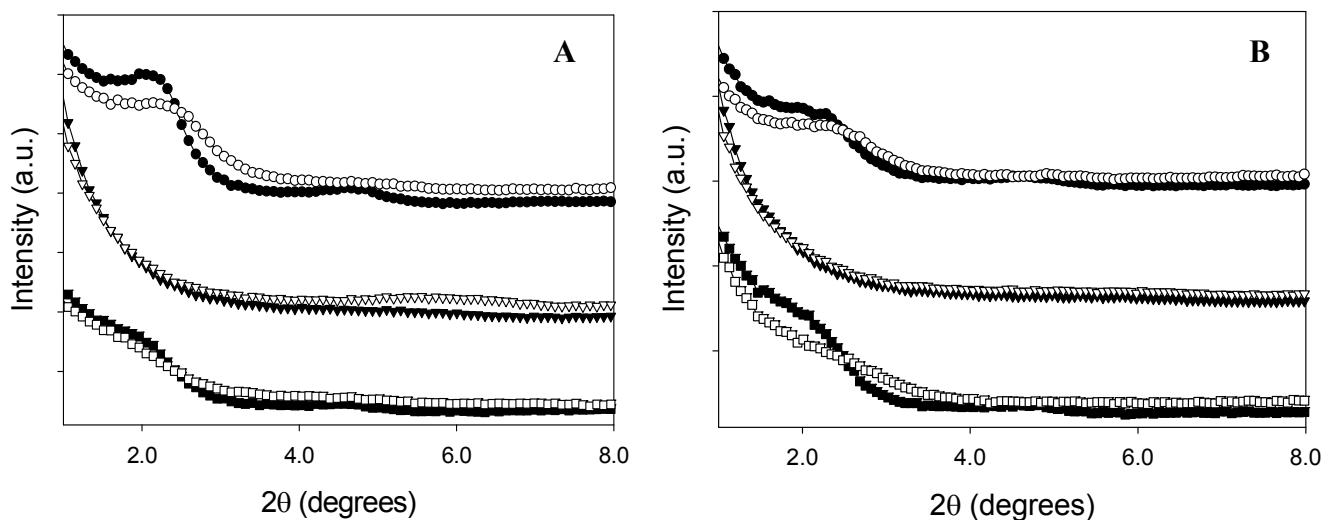


**Figure 4:** SAXS profiles of 5wt% polymerizable organoclay dispersed in NPGDA (A) and HDDA (B). C14MA-organoclay (circles), PM1-organoclay (triangles) and PSH2-organoclay (squares) are shown with filled symbols representing uncured samples and empty symbols indicate polymerized samples.

Incorporating organoclays into polymer composites may alter the mechanical properties of the resulting substrates because of the higher modulus of clay in comparison to the polymer. To investigate how polymerizable organoclays influence mechanical properties of clay-photopolymer nanocomposites, DMA studies were conducted on 3wt% organoclay composite samples. Figure 5 shows changes in Young's modulus of organoclay-polymers as compared to the pristine polymer. Adding the non-polymerizable Cloisite 15A leads to significant decreases in Young's modulus of both NPGDA and HDDA composites. The polymerizable organoclays only offer slight improvements in the Young's modulus compared to the pristine polymer. Adding C14MA-organoclay to NPGDA results in approximately the same modulus as observed for Cloisite 15A. However, a significant improvement occurs when C14MA-organoclay is dispersed in HDDA. While a 35% decrease in modulus is observed on adding the organoclay to NPGDA, a 10% increase in modulus compared to HDDA is observed with C14MA-organoclay. The Young's modulus of C14MA-organoclay-HDDA system shows only a 10% increase over the pristine polymer. PM1-organoclay systems are the most consistent, with ca. 5-10% increase in modulus in both NPGDA and HDDA nanocomposites. The trends in the modulus of PM1-organoclay systems are very consistent with other reports in that exfoliating organoclays lead to improvements in mechanical properties of the resulting nanocomposites.

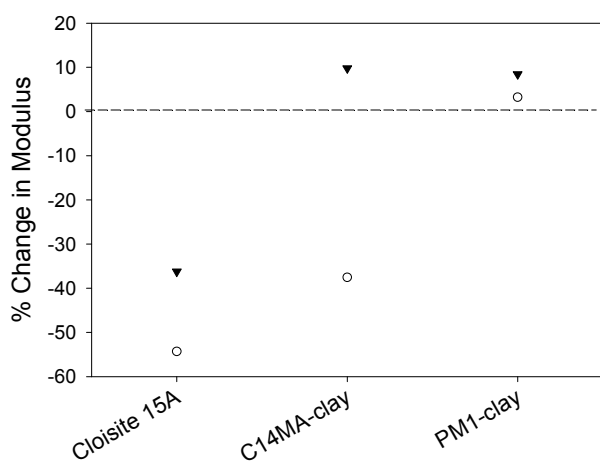


**Figure 5:** Percent change in Young's modulus of 3wt% organoclay dispersed in NPGDA (○) or HDDA (▼) as compared to the pristine polymer (dashed line).

However, the observed behavior is contrary to observations in other systems reported elsewhere.<sup>6-11</sup> These differences may stem from the morphology of the polymer utilized in generating the nanocomposites. For these photopolymers, high cross-link density inherent in the polymers leads to mechanically robust systems that may not benefit from addition of clay nanoparticles. More likely, introducing intercalated organoclay into the polymer host disrupts the polymer network and lead to the observed decreases in mechanical properties. Further studies are underway to elucidate the influence of crosslink density on the mechanical properties of photopolymer nanocomposites. To understand the evolution of mechanical properties of these systems, photopolymerization kinetics can be used to evaluate the influence of polymerizable organoclays on reaction behavior

of the filled systems. Photo-differential scanning calorimetry (photo-DSC) is a versatile instrument for evaluating the polymerization behavior *in situ*. The rate of polymerization is correlated to the amount of heat evolved as a function of time for a particular system.

Figure 6a shows a typical photo-DSC profile as a function of time for *in situ* monitoring of polymerization rates. The exotherm peak is related to the maximum rate of polymerization, while the area under the curve relates to the functional group conversion. A plot of the maximum rate of polymerization as a function of organoclay concentration is shown for an organoclay-HDDA system in Figure 6b. Increasing concentration of the non-polymerizable organoclay leads to a monotonous decrease in the maximum rate of polymerization. In comparison, incorporating both C14MA- and PM1-

organoclay induce different polymerization dynamics in the system. Though lower maximum polymerization rates occur in the polymerizable organoclay systems, the rate of polymerization remains approximately constant with clay loadings between up to 10wt%.

Lower polymerization rates would be expected in the non-polymerizable organoclay system because of light scattering and/or absorption by the intercalated clay aggregates. The same could be said of the C14MA-organoclay system since intercalated domains remain in the formulation. However, at higher concentrations, potential decreases in termination due to immobilization of some of the reactive species (surfactants) could lead to the observed polymerization behavior. In addition to decreased termination events, exfoliated PM1-organoclay potentially allows easier access to the immobilized reactive species and accounts for the observed polymerization behavior in Figure 6b. Modifying clay surfaces with polymerizable surfactants therefore, leads to enhanced exfoliation and photopolymerization rates.

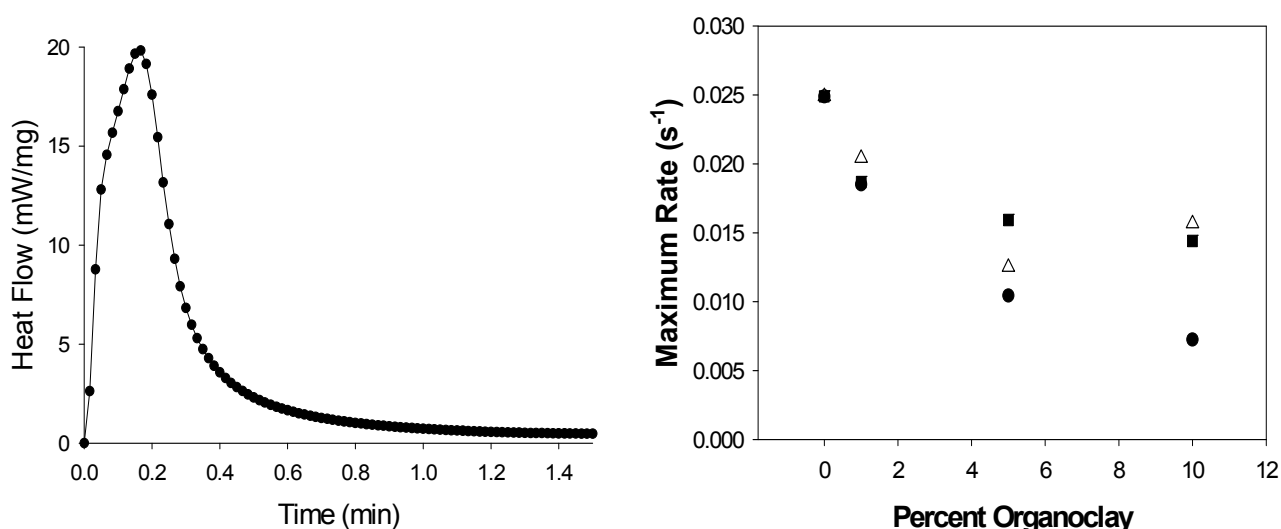


**Figure 6:** a) Typical photo-DSC exotherm as a function of time. B) Maximum polymerization rate versus concentration for Cloisite 15A (●), C14MA-organoclay (Δ) and PM1-organoclay (■) dispersed in HDDA. Samples contain 0.1wt% DMPA and were polymerized at 3 mW/cm<sup>2</sup>.

## Conclusion

Quaternary ammonium surfactants that have been modified with methacrylate and thiol functionalities were utilized in lyophilizing clay nanoparticles. The polymerizable organoclays are easily characterized by FTIR instrumentation. Polymerizable organoclays disperse readily under mild conditions in various photopolymerizable systems. The enhanced dispersion is a result of increased compatibility with the bulk monomer as well as intragallery polymerization due to presence of reactive species anchored onto the clay surfaces. Exfoliated organoclays only minimally improves mechanical properties of the nanocomposite over pristine polymers. However, without the polymerizable species, organoclays intercalate in the polymer and result in drastically lower composite mechanical properties. Photopolymerization rate decreases slightly and plateaus with increasing concentration of polymerizable organoclay while traditional organoclays decreases photopolymerization rates significantly with higher loading.

## Acknowledgements

The authors gratefully acknowledge financial support from the National Science Foundation (CTS-0626395) and the I/UCRC Center for Fundamentals and Applications of Photopolymerization.

## References

1. Parak, W. J., Gerion, D., Zanchet, D., Woerz, A. S., Pellegrino, T., Micheel, C., Williams, S. C., Seitz, M., Bruehl, R., Bryant, Z., Bustamante, C., Bertozzi, C. R., Alivisatos, A. P. *Chem. Mater.* **2002**, 14, 2113-2119
2. Alivisatos, P. *Pure. Appl. Chem.* **2000**, 72, 3-9.
3. Lee, J., Sundar, V. C., Heine, J. R., Bawendi, M. G., Jensen, K. F. *Adv. Mater.*, **2000**, 12, 1102.
4. Harrison, M. T., Kershaw, S. V., Burt, M. G., Rogach, A. L., Komowski, A., Evchmuller, A., Weller, H. *Pure Appl. Chem.*, **2000**, 72, 295
5. Usuku, A.; Kojima, Y.; Kawasumi, M.; Okada, A.; Fukushima, Y.; Kurauchi, T., Kamigaito, O. *J. Mater. Res.* **1993**, 8 1185
6. Kato, M., Usuki, A., Okada, A., *J Appl Polym Sci* **1997**, 66,1781.
7. Okada, A., Kawasumi, M., Kurauchi, T., Kamigaito, O. *ACS Polym. Prepr.* **1987**, 28, 447
8. Alexandre, M.; Dubois, P. *Mater. Sci. Eng.* **2000**, 28, 1.
9. Vaia, R. A.; Giannelis, E. P. *Macromol.* **1997**, 30, 7990.
10. Decker, C.; Keller, L.; Zahouily, K.; Benfarhi, S. *Polymer* **2005**, 46, 6640.
11. Uhl F. M.; Davuluri S. P.; Wong S. C.; Webster D. C. *Chem. Mater.* **2004**, 6, 1135.
12. Yebassa, D., Balakrishnan, S., Feresenbet, E., Raghavan, P., Start, R., Hudson, S. D. *J. Polym. Sci. A: Polym. Chem.* **2004**, 42, 1310-1321
13. Giannelis, E. P., Bergman, J. S., Chen, H., Thomas, M. G., Coates, G. W. *Chem Commun* **1999**, 21, 2179–2180.
14. Pinnavaia, T. J., Wang, Z. *Chem Mater* **1998**, 10, 3769–3771.
15. Tabtiang, A.; Lumlong, S.; Venables, R. A. *Polym.-Plast. Technol. Eng.* **2000**, 39, 293.
16. Huang, X. Y.; Brittain, W. J. *Macromol.* **2001**, 34, 3255
17. Xie, W.; Gao, Z. M.; Pan, W. P.; Hunter, D.; Singh, A.; Vaia, R. *Chem. Mater.* **2001**, 13, 2979.
18. Bhiwankar, N. N.; Weiss, R. A. *Polymer* **2006**, 47, 6684.
19. Horsch, S.; Serhatkulu, G.; Gulari, E.; Kannan, R. M. *Polymer* **2006**, 47, 7485.
20. Hasegawa, N.; Okamoto, H.; Kato, M.; Usuki, A.; Sato, N. *Polymer* **2003**, 44, 2933.
21. Weimer, M. W.; Chen, H.; Giannelis, E. P.; Sogah, D. Y. *J. Am. Chem. Soc.* **1999**, 121, 1615.
22. Jianbo, D.; Sogah, D. Y. *Macromol.* **2006**, 39, 5052.
23. McGrath, K. M.; Drummond, C. J. *Colloid Polym. Sci.* **1996**, 274, 612.
24. Joynes, D.; Sherrington, D. C. *Polymer*, **2006**, 37, 1453.
25. Lagaly, G.; Beneke, K. *Colloid Polym. Sci.* **1991**, 269, 1198.
26. Katti, K. S.; Sikdar, D.; Katti, D. R.; Ghosh, P.; Verma, D. *Polymer* **2006**, 47 403-414.
27. DePierro, M.; Guymon, C. A. *Macromol.* **2006**, 39, 617-626